Journal of Science and Technology (JST)
Volume 2, Issue 2, March - April 2017, PP 01-13
www.jst.org.in

Firefly Algorithm Based Reactive Power Control of an Isolated Wind-Diesel Hybrid Power System

Syed Shahbazuddin
(Assistant Professor, Vaagdevi Engineering College, Waranngal)

Abstract *: This work proposes the reactive power control of an isolated hybrid power system. The system consists of a synchronous generator incorporated for diesel engine system, induction generator incorporated for the wind energy conversion system. In order to minimize the surplus reactive power requirement of the system, FACTS device SVC is employed in the system. For a robust voltage control of the system, controllers of proportional and integral type have been incorporated for AVR of the excitation system of the synchronous generator and SVC. The controller parameters are optimized using firefly algorithm (FA). The dynamic response of the system has been tested for different degrees of load disturbances plus variable nature of the wind system.*

Keywords *- Diesel engine generator (DEG), Induction generator (IG), Firefly Algorithm (FA), Static VAr compensator (SVC), Synchronous generator (SG).*

I. INTRODUCTION

Rapid increase for the demand of electrical energy, increased global environmental concern by the usage of fossil fuels, and tight constraints on the construction of transmission systems has triggered the implementation of isolated power systems. Of particular interest are the renewable energy sources with free energy. These renewable energy sources are emission free, sustainable, eco-friendly and different types of renewable energy sources are accessible depending on the location of the loads. But the major drawback is that they are intermittent in nature [5].Hence, to boost the capacity, improve the continuity and reliability of the supply, these renewable energy systems are integrated with conventional systems such as diesel energy systems. This diesel energy system will act as a back bone for total isolated system. This combination of conventional and renewable energy systems is called as hybrid power systems [14].

In an isolated system, as the generation and consumption of electrical energy are in proximity to each other, so the reactive power requirement has direct effect on generators. This problem becomes more severe in hybrid power systems, which affect the power quality and the voltage stability of the system [6]. Hence to supply the additional reactive power, required by the load along with induction generator of the system, SVC has been incorporated.

The met heuristic algorithms that are based on the swarm intelligence have attracted much attention in last few years [9]. Firefly algorithm, developed by X. S. Yang, a swarm intelligence based algorithm is based on the flashing pattern of tropical fireflies [8]. It was shown that the new firefly algorithm is superior to both PSO and GA in terms of efficiency in finding the global optimum and success rate [8].

FA is superior to other swarm intelligence techniques in two aspects that are automatic subdivision and the ability to deal with multimodality. This implies that the whole fireflies categorize themselves into subgroups and each group swarm around each local optimum. Among all these, the global best is chosen. Secondly, this subdivision allows fireflies to find all the optima in parallel. These advantages make FA suitable to deal with continuous and multimodal problems and combinational optimization as well [8].

In this work, the integral square error criterion is considered to calculate the optimal gain settings of controller parameters of SVC and AVR of synchronous generator.

The objectives of the present work are summarized as follows.

(i) Performance of the system with and without the incorporation of SVC.
(ii) Optimizing the gains of PI controllers of SVC and AVR of the system using FA.
(iii) Investigate the performance of the system with the optimized controller parameters for step changes in reactive power load and/or wind power input to the IG.

This paper is structured as follows: Mathematical modeling is presented in section II. Problem formulation is done in section III. Simulation results and analysis of 3 different cases have been carried out in section IV, V respectively and section VI covers the conclusions.

II. MATHEMATICAL MODELING OF COMPONENTS OF THE WIND-DIESEL HYBRID POWER SYSTEM

A hybrid system consisting of wind energy system (150 kW), DEG (150 kW) and load (250 kW) is considered for reactive power analysis as shown in fig.1. The diesel engine system is integrated with synchronous generator and the wind energy system is coupled with an induction generator for electro mechanical energy conversion [1-3] [5-7].

The reactive power required by the system load and also the induction generator cannot be supplemented alone by the SG. Even an oversized generator for supplying reactive power may prove to be uneconomical and inefficient under light loaded conditions [1]. As this reactive power compensation is a major factor to be considered for better voltage stability and power quality, An SVC is incorporated, that can supply fast and continuous reactive power [4].

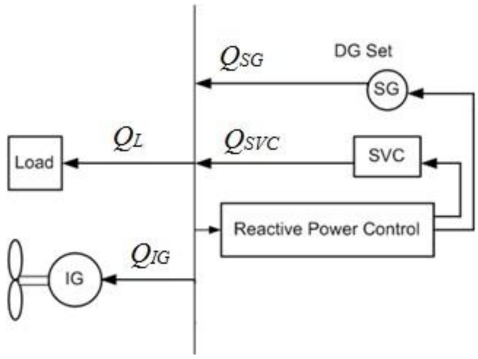

Figure 1. Block diagram of wind-diesel hybrid energy system

From the knowledge of various sources of generation and load, the power balance equations of the system is given by [2],

$$P_{SG} + P_{IG} = P_L \quad (1)$$

$$Q_{SG} + Q_{SVC} = Q_L + Q_{IG} \quad (2)$$

The mathematical modeling of the system is based on [1-7].

Under equilibrium conditions, reactive power supplied by the SG, SVC is balanced by the reactive power absorbed by IG and system load [1-7]. When the system is subjected to an incremental reactive power load ΔQ_L, due to the action of AVR of the SG and SVC, the reactive power generated in the system increases by an amount of ($\Delta Q_{SG}+\Delta Q_{SVC}$). Due to the change in the voltage of the system, reactive power required by the load and the induction generator also changes. Hence, the net surplus reactive power of the system is given by, $\Delta Q_{SG}+\Delta Q_{SVC}-\Delta Q_L-\Delta Q_{IG}$. This surplus will attribute to the increase in system voltage in two ways [1-7]:

(1) By increasing the electromagnetic energy absorbed (E_M) by the IG at the rate $\frac{d}{dt}(\Delta E_M)$

(2) Increase of reactive power consumption by the load at the rate of D_V.

This is mathematically expressed as,

$$\Delta Q_{SG} + \Delta Q_{SVC} - \Delta Q_{Load} - \Delta Q_{IG} = \frac{d}{dt}(\Delta E_M) + D_V \Delta V \quad (3)$$

This excess reactive power leading to increase in system voltage in Laplace form is given by [1-3] [4-7] [11-13],

$$\Delta V(s) = \frac{K_V}{1+sT_V}[\Delta Q_{SG}(s) + \Delta Q_{SVC}(s) - \Delta Q_{Load}(s) - \Delta Q_{IG}(s)] \quad (4)$$

Where $T_V = 2H_r / D_V V^o$ and $K_V = 1/D_V$ are the system time constant and gain, respectively and $D_V = \frac{\partial Q_L}{\partial V}$.

The SG of diesel engine system employs an IEEE type-1 excitation system [13].the equations pertaining to change in field voltage for changes in system terminal voltage are given by,

$$\Delta E_{fd}(s) = \frac{1}{K_E + sT_E} \Delta V_a(s) \quad (5)$$

$$\Delta V_a(s) = \frac{K_A}{1+sT_A} \Delta V_a^{'}(s) \quad (6)$$

A PI controller provided with the AVR for a better voltage control i.e.

$$\Delta V_a(s) = \left(K_{pAVR} + K_{iAVR}/s\right)[-\Delta V(s) - \frac{K_F}{T_F}\Delta E_{fd}(s) + \Delta V_{ref}(s)] \quad (7)$$

$$\Delta V_f(s) = \frac{K_F / T_F}{1+sT_F} \Delta E_{fd}(s) \quad (8)$$

The flux linkage equations which governs the changes in SG terminal voltage according to changes in field voltage is given by [2]

$$\Delta E_q^{'}(s) = \frac{1}{(1+sT_G)} K_1 \Delta E_{fd}(s) + K_2 \Delta V(s) \quad (9)$$

Where $K_1 = \frac{x_d^{'}}{x_d}$, $K_2 = \{(x_d - x_d^{'})\cos\delta\}/x_d$ and $T_G = T_{do}^{'} \frac{x_d^{'}}{x_d}$

The expression for reactive power required by SG under transient conditions is given by,

$$Q_{SG} = \frac{K_q^{'} V \cos\delta - V^2}{x_d^{'}} \quad (10)$$

For small perturbation, (10) can be written as,

$$\Delta Q_{SG} = \frac{V\cos\delta}{x_d^{'}} \Delta E_q^{'} + \frac{E_q^{'}\cos\delta - 2V}{x_d^{'}} \Delta V \quad (11)$$

Equation (11) in Laplace form is written as [2],

$$\Delta Q_{SG}(s) = K_3 \Delta E_q^{'}(s) + K_4 \Delta V(s) \quad (12)$$

Where $K_3 = \frac{V\cos\delta}{x_d^{'}}$ and $K_4 = \frac{E_q^{'}\cos\delta - 2V}{x_d^{'}}$

Considering equivalent circuit model of the IG for its mathematical modeling, which makes it more suitable for multi machine system, the reactive power absorbed by the IG is given by [11],

$$Q_{IG}(s) = \frac{V^2 X_{eq}}{R_Y^2 + X_{eq}^2} \tag{13}$$

Under constant slip conditions, reactive power absorbed for small perturbation of voltage is given by [1-3] [4-7],

$$\Delta Q_{IG}(s) = K_5 \Delta V(s) \tag{14}$$

Where $K_5 = \frac{2VX_{eq}}{R_Y^2 + X_{eq}^2}$ and $R_Y = R_P - R_{eq}$, $R_P = R_2'/s$

Under variable slip conditions, reactive power absorbed [11] is given by,

$$\Delta Q_{IG}(s) = K_6 \Delta P_{IW}(s) + K_7 \Delta V(s) \tag{15}$$

Where $K_6 = \frac{Q_{IG}}{P_{IW} - P_{closs} - \frac{1}{2}\frac{V^2}{R_Y}}$ (16)

$$K_7 = \frac{2V}{R_Y^2 + X_{eq}^2}\left[X_{eq} - \frac{R_P Q_{IG}}{P_{IW} - P_{closs} - \frac{1}{2}\frac{V^2}{R_Y}}\right] \tag{17}$$

The SVC generally comprised of a fixed capacitor in shunt with a Thyristor controlled reactor is considered for reactive power compensation as shown in fig. 2.

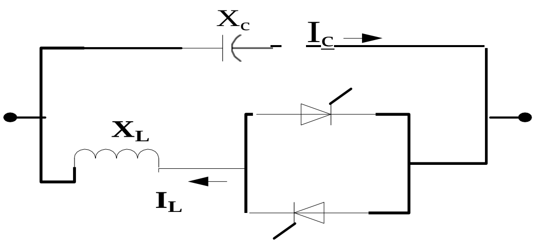

Figure. 2. Equivalent circuit of an SVC.

Reactive power supplied by the SVC is given by [1-3] [4-7] [11],

$$Q_{SVC} = B_{SVC} V^2 \tag{18}$$

For a small disturbance, (18) is given by [1-3] [4-7] [11],

$$\Delta Q_{SVC} = 2VB_{SVC}\Delta V + V^2 \Delta B_{SVC} \tag{19}$$

$$= K_6 \Delta V + K_7 \Delta B_{SVC} \tag{20}$$

Where $K_6 = 2VB_{SVC}$ and $K_7 = V^2$ (21)

The expressions for SVC having a PI type of controller for firing angle delay, phase sequence zero crossing delay are given by [2]

$$\Delta B_{SVC}(s) = \frac{1}{1+sT_d}\Delta B'_{SVC}(s) \quad (22)$$

$$\Delta B'_{SVC}(s) = \frac{K_\alpha}{1+sT_\alpha}\alpha(s) \quad (23)$$

$$\Delta\alpha(s) = \left(K_{pSVC} + \frac{K_{iSVC}}{s}\right)\left(\Delta V_{ref}(s) - V(s)\right) \quad (24)$$

Using above equations, the transfer function model of wind-diesel system has been developed as shown in fig. 3.

III. PROBLEM FORMUATION

To provide a robust voltage control, PI controller parameters of SVC and AVR are to be optimized simultaneously. The integral square error (ISE) criterion is considered to calculate the optimum gain parameters of SVC, AVR which is given by,

$$J = \int_0^T \left(|\Delta V|\right)^2 dt \quad (25)$$

Where T is the simulation time and ΔV is the voltage deviation. The objective is to minimize the performance index J by optimizing controller parameters. The objective function is subjected to following constraints,

$$K_{pSVC}^{min} \le K_{pSVC} \le K_{pSVC}^{max} \quad (26)$$

$$K_{iSVC}^{min} \le K_{iSVC} \le K_{iSVC}^{max} \quad (27)$$

$$K_{PAVR}^{min} \le K_{pAVR} \le K_{PAVR}^{max} \quad (28)$$

$$K_{iAVR}^{min} \le K_{iAVR} \le K_{iAVR}^{max} \quad (29)$$

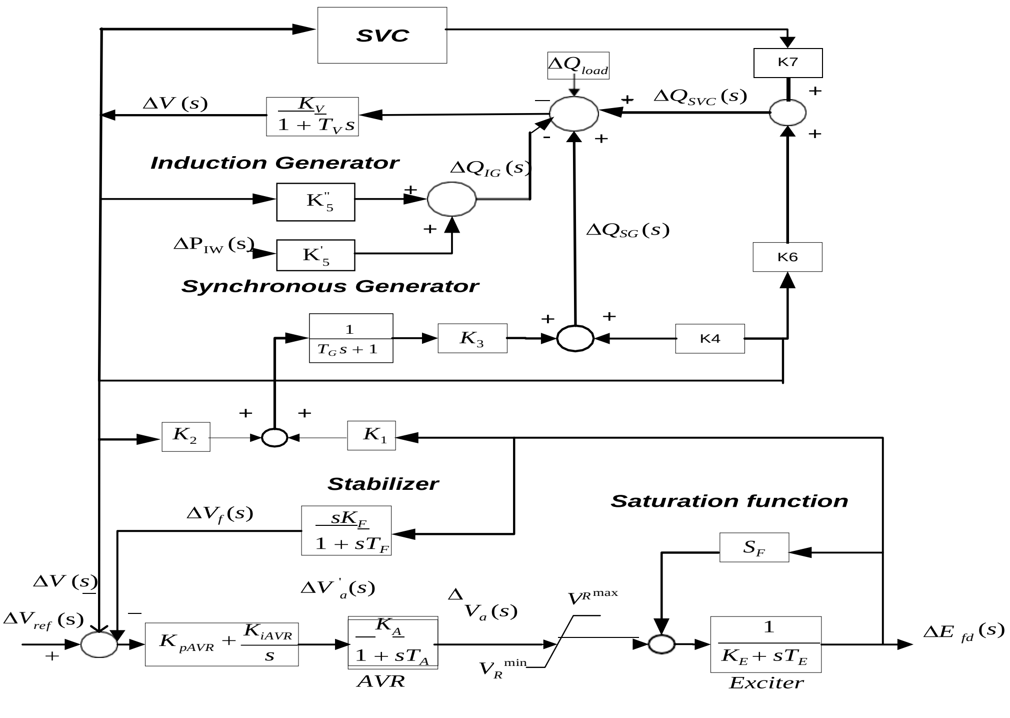

Figure 3. Transfer function model of the proposed system

Controller parameters are optimized using Firefly Algorithm. It is very efficient in dealing with multi modal and global optimization problems [8]. The tuned parameters of Firefly optimization algorithm are presented in Table 1.

Table 1. Parameters of FA

Parameter	Value
Alpha	0.25
Beta	0.20
Gamma	1.00
No. Of Iterations	100
No. Of Fireflies	20

The first paragraph under each heading or subheading should be flush left, and subsequent paragraphs should have a five-space indentation. A colon is inserted before an equation is presented, but there is no punctuation following the equation. All equations are numbered and referred to in the text solely by a number enclosed in a round bracket (i.e., (3) reads as "equation 3"). Ensure that any miscellaneous numbering system you use in your paper cannot be confused with a reference [4] or an equation (3) designation.

IV. RESULTS AND ANALYSIS

Analysis of the proposed system under various loading conditions and/or input wind power is discussed in this section.

Case 1: Performance of the system without SVC under step Changes in Reactive power loading Q_{Load} and Constant Input Wind Power P_{IW}

Under normal operating conditions, reactive power absorbed by the load is 0.75p.u. To investigate the transient response of the system without employing SVC, step change in Q_{Load} is considered keeping the mechanical input to the wind system constant. Q_{Load} rises by 10% of its nominal value 0.75 p.u. (i.e., ΔQ_{Load} =0.075) as shown in fig. 4(a). Transient response of the voltage deviation with and without employing the SVC has been shown in fig. 4(b). The voltage deviation of the system is not converging even after certain time interval the disturbance in reactive power load is given. The reactive power supplied by AVR alone is unable to supplement the additional reactive power load in the system.

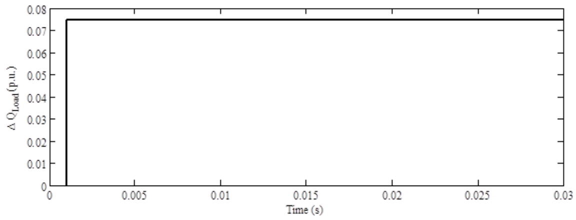

Figure 4(a) Step change in reactive power load (Q_{Load}) at constant input wind power (P_{IW})

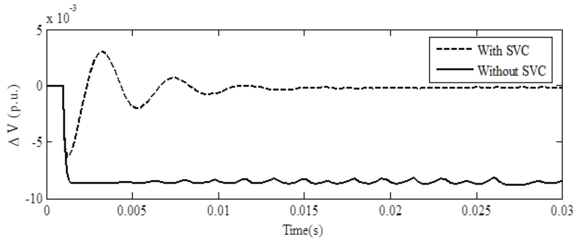

Fig. 4(b) Voltage deviation of the hybrid system with and without the SVC for a step change in reactive power loading (case 1)

Case 2: Performance of the system with SVC under Step Disturbance Q_{Load} and Constant P_{IW}

In this case, the transient response of the system with SVC under step changes of reactive power absorbedby the load is analyzed. Step changes in reactive power consumed by the load have been shown in Fig. 4(a). The mechanical input (i.e. P_{IW}) to the induction generator is considered constant in this case. The voltage deviation of the system has been shown in Fig. 4(c). Due to the action of AVR and SVC, the voltage deviation has settled very quickly within a time period of 0.015s. The transient response of ΔQ_{SVC}, ΔQ_{SG} and ΔQ_{IG} for corresponding load disturbance has been shown in Fig. 4(d-e) respectively. The maximum voltage deviation observed in this case is about 0.298%, which is quite below the IEEE requirements limit. Table 4.1(a) presents the parameters of the PI controller employed with SVC and AVR in different case studies. The voltage deviation and transient response of each component in case 2 is shown in Table 5(b).

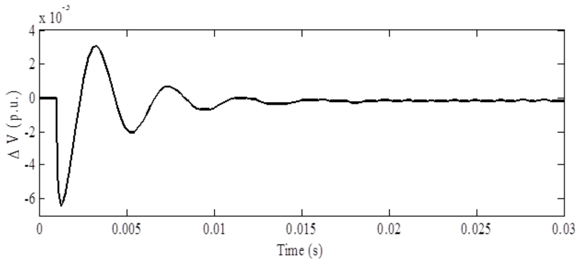

Figure 4(c) Voltage deviation of the system for step changes in reactive power loading (case 2).

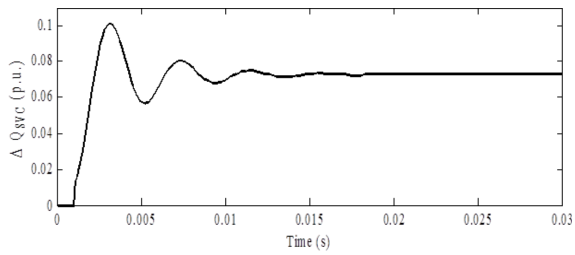

Figure 4(d) Transient response of SVC for step changes in reactive power loading (case 2).

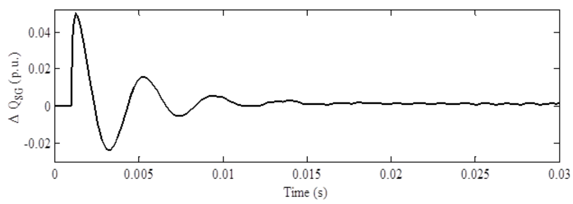

Figure 4(d) Transient response of SG for step changes in reactive power loading (case 2).

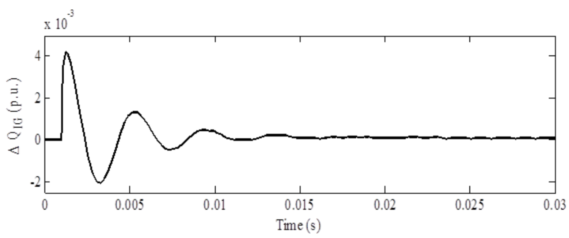

Figure 4(e) Transient response of IG for step changes in reactive power loading (case 2).

Case 3: Performance analysis of the system with SVC, under Step Changes in Q_{Load} as well as P_{IW}

The transient response of the system under step change in Q_{Load} as well as P_{IW} has been investigated in this case. These step changes are shown in Fig. 4(f). The deviation in system voltage corresponding to given disturbances is shown in Fig. 4(g). The transient responses of ΔQ_{SVC}, ΔQ_{SG} and ΔQ_{IG} corresponding to changes in Q_{Load} and P_{IW} are shown in Fig. 4(h-j) respectively. Voltage deviation and transient response of each component in case 3 is shown in Table 5(c).

A sensitivity analysis has been carried out to check the robustness of FA optimized controller parameters. Controllers' gain parameters obtained in case 2 has been substituted for the controller parameters of case 3. Deviation in voltage is shown in Fig. 4(k). The response shows that the FA optimized PI controller parameters are quite robust and need not be adjusted further for changes in the disturbance conditions.

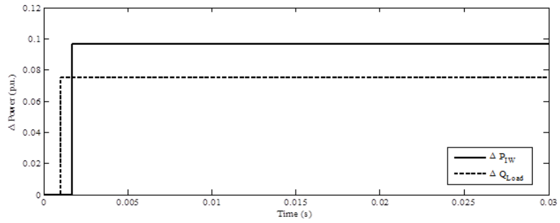

Figure 4(f) Step changes in reactive power loading (Q_{Load}) as well as input wind power (P_{IW}) (case3).

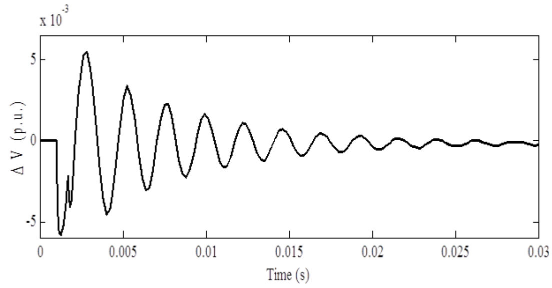

Figure 4(g) Transient response of voltage for step changes in reactive power loading (Q_{Load}) as well as input wind power (P_{IW}) (case3).

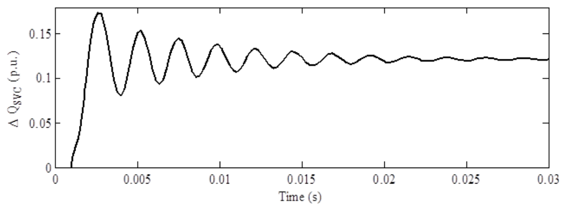

Figure 4 (h) Transient response of SVC for step changes in reactive power loading (Q_{Load}) as well as input wind power (P_{IW}) (case 3).

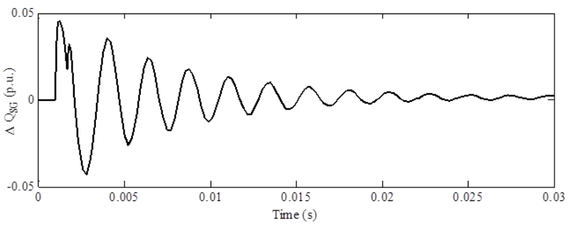

Figure 4(i) Transient response of SG for step changes in reactive power loading (Q_{Load}) as well as input wind power (P_{IW}) (case 3).

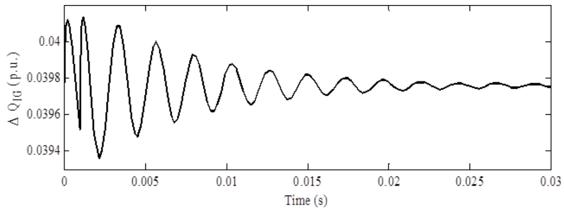

Figure 4(j) Transient response of IG for step changes in reactive power loading as well as input wind power (case 3).

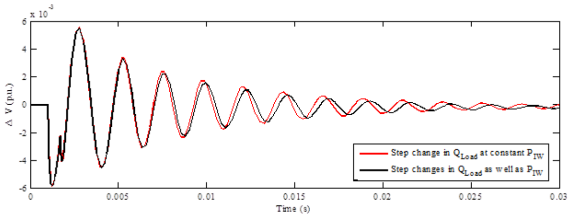

Figure 4(k) Comparative performance of FA optimized PI controller under step changes in Q_{Load} (case2) vis-à-vis FA optimized PI controller under step changes in Q_{Load} and P_{IW} (case 3) in terms of voltage deviations.

Case 4: Performance analysis of the system with SVC, under Random Variations in Q_{Load} as well as P_{IW}

The transient response of the system under random variations in Q_{Load} as well as P_{IW} (as shown in Fig. 4(l), Fig. 4(m)) has been investigated in this case. The system voltage deviation under such disturbances is shown in Fig. 4(n). The transient responses of ΔQ_{SVC}, ΔQ_{SG} and ΔQ_{IG} corresponding to changes in Q_{Load} and P_{IW} are shown in Fig. 4(o-q) respectively. Voltage deviation and transient response of each component in case 4 is shown in Table 5(d).

Another sensitivity analysis has been carried out to check the robustness of FA optimized controller parameters. Controllers' gain parameters obtained in case 2 has been substituted for the controller parameters of case 4. The voltage deviation is shown in Fig. 4(r). The response shows that the FA optimized PI controller parameters are quite robust and need not be changed for a wide range of disturbance in reactive power load and wind input power.

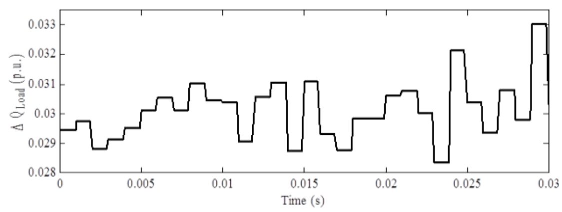

Figure 4(l) Random variation of reactive power loading Q_{Load} (case 4).

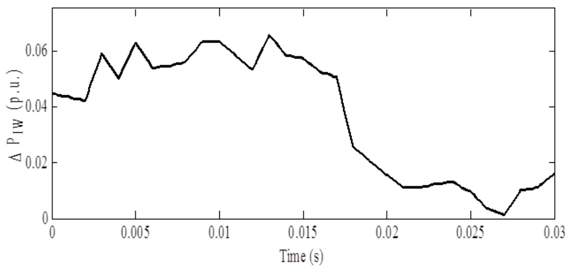

Figure. 4(m) Random variation in mechanical input to the wind turbine PIW (case 4)

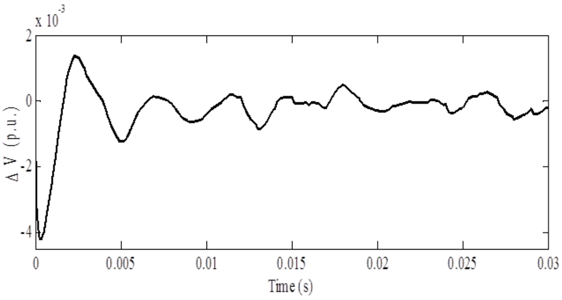

Figure. 4(n) Transient response of voltage for random variation of reactive power load (Q_{Load}) as well as input wind power (P_{IW}) (case 4).

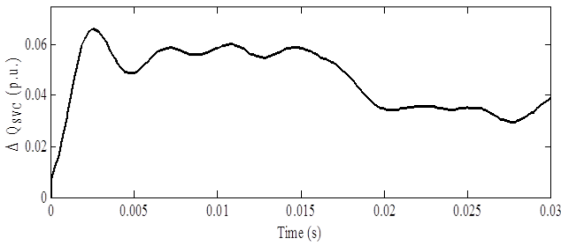

Figure 4(o) Transient response of SVC for random variation of reactive power load (Q_{Load}) as well as input wind power (P_{IW}) (case 4).

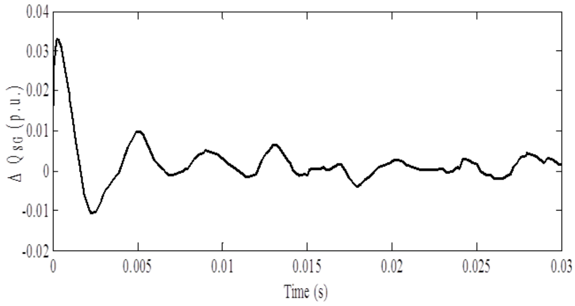

Figure 4(p) Transient response of SG for random variation of reactive power load (Q_{Load}) as well as input wind power (P_{IW}) (case 4).

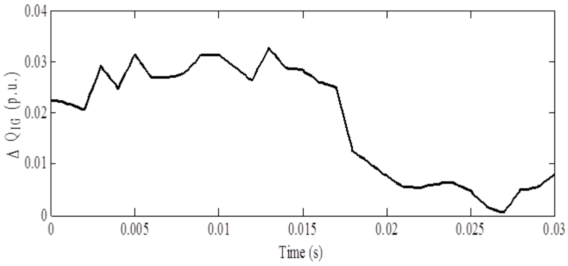

Figure 4(q) Transient response of IG for random variation of reactive power load (Q_{Load}) as well as input wind power (P_{IW}) (case 4).

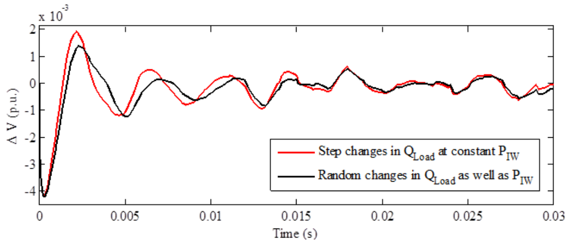

Figure 4(r) Comparative performance of FA optimized PI controller under step changes in Q_{Load} (case2) vis-à-vis FA optimized PI controller under random changes in Q_{Load} , P_{IW} (case 4) in terms of voltage deviations.

V. ANALYSIS OF THE RESULTS

Table 5(a) gives the gain parameters of controllers employed SVC and AVR of the wind-diesel hybrid power system.

Table5(a) Gain parameters of PI controllers employed with SVC and AVR in three different case 2, 3, 4 respectively

S. No	Gain	Case 2	Case 3	Case 4
1	K_{pSVC}	142.1709	483.312	108.520
2	K_{iSVC}	2033.90	294.63	2024.220
3	K_{pAVR}	120.039	117.920	76.688
4	K_{iAVR}	97.373	109.321	141.257

Following tabular forms gives the data associated with the response of each component of the system when it is subjected to different types of reactive power loading conditions and/or mechanical input to the induction generation of wind energy system as described in case 2, case 3, case 4 respectively.

Table 5(b) Transient responses of different components of the system for 10% of reactive load perturbation and constant slip conditions (case 2)

S. No	Response	Peak Undershoot	Peak Overshoot	Settling Time(sec)
1	ΔV	$-6.379*10^{-3}$	$3.068*10^{-3}$	0.01807
2	ΔQ_{SVC}	0.05701	0.1007	0.01714
3	ΔQ_{SG}	-0.02402	0.0499	0.01714
4	ΔQ_{IG}	$-1.984*10^{-3}$	$4.248*10^{-3}$	0.01523

Table 5(c) Transient responses of different components of the system for 10% of reactive load perturbation and variable slip conditions (case 3)

S. No	Response	Peak Undershoot	Peak Overshoot	Settling Time(sec)
1	ΔV	$-5.809*10^{-3}$	$5.478*10^{-3}$	0.0282
2	ΔQ_{SVC}	0.08095	0.1744	0.02846
3	ΔQ_{SG}	-0.04287	0.04544	0.0292
4	ΔQ_{IG}	0.03436	0.04013	0.0286

Table 5(d) Transient responses of different components of the system for random variations in reactive power load as well as mechanical input to the IG (case 4)

S. No	Response	Peak Undershoot	Peak Overshoot
1	ΔV	$-4.185*10^{-3}$	$1.374*10^{-3}$
2	ΔQ_{SVC}	0.0297	0.06605
3	ΔQ_{SG}	-0.010177	0.03291
4	ΔQ_{IG}	$5.522*10^{-4}$	0.03268

From the time domain simulation results of the wind-diesel hybrid system, following can be concluded:

The net change in the reactive power of the system and the voltage deviation when the system is subjected to reactive power load disturbances and wind input variations are minimized with the incorporation of the SVC. Though the AVR of the SG is supplying the reactive power under transient conditions, major amount of the surplus reactive power is compensated by SVC only both under transient and steady state conditions.

As in case 4, when the system is subjected to random variations in reactive power loading as well as wind power input, the voltage deviation and other transient responses are sufficiently within the limits as show in Table 5(d).

VI. CONCLUSION

In this paper, automatic reactive power control of an isolated system consisting of wind, diesel engine systems is considered. In addition to the reactive power provided by AVR, SVC provides the major portion of required reactive power. A complete dynamic model of the system has been developed to study the effect of load disturbances and/ or change in P_{IW}. To ensure the coordinated control, the parameters of SVC and AVR controllers are optimized simultaneously considering uncertainties as mentioned in the case studies. . It is observed that major part of the reactive power is provided by the SVC only. Reactive power is supplied by SG under transient conditions only. FA is applied in optimizing the controller parameters. The significant contributions from this work are as follows:

The transient study for voltage deviations of the hybrid system without SVC has been carried out for step changes in Q_{Load}. Results indicated that the voltage deviations are considerably large and AVR alone are not capable of maintaining the voltage at the desired level. In order to provide a better voltage control, system is incorporated with an SVC.

The dynamic responses show that coordinated control of SVC and AVR with their gains tuned by Firefly algorithm can provide improved dynamic performance of the hybrid energy system in containing the voltage deviation.

REFERENCES

[1] R. C. Bansal, "ANN based reactive power control of isolated wind diesel micro-hydro hybrid power systems," *International Journal of Modelling, Identification and Control*, vol. 6, no.3, 2009, pp. 196-204.

[2] R. C. Bansal, "Automatic Reactive-Power Control of Isolated Wind Diesel Hybrid Power Systems," *IEEE Trans. on Industrial Electronics*, vol. 53, no. 4, August 2006, pp. 1116-1126.

[3] R. C. Bansal, T.S. Bhatti, and D.P. Kothari, "A novel mathematical modelling of induction generator for reactive power control of isolated hybrid power systems," *Int. J. Model. Simul.*, vol. 24, no. 1, 2004, pp. 1-7.

[4] Sharma, Pawan, Waldemar Sulkowski, and Bjarte Hoff, "Dynamic stability study of an isolated wind-diesel hybrid power system with wind power generation using IG, PMIG and PMSG: A comparison," *International Journal of Electrical Power & Energy Systems 53*, 2013, pp. 857-866.

[5] Sharma, Pawan, and T. S. Bhatti, "Performance investigation of isolated wind–diesel hybrid power systems with WECS having PMIG," *Industrial Electronics, IEEE Transactions on* 60, no.4, 2013, pp.1630-1637.

[6] Sharma, Pawan, T. S. Bhatti, and K. S. S. Ramakrishna. "Control of reactive power of autonomous wind-diesel hybrid power systems," *Power Electronics, Drives and Energy Systems (PEDES) & 2010 Power India, 2010 Joint International Conference on*. IEEE, 2010, pp. 1-6.

[7] Vachirasricirikul Sitthidet, Issarachai Ngamroo, and Somyot Kaitwanidvilai, "Coordinated SVC and AVR for robust voltage control in a hybrid wind-diesel system," *Energy Conversion and Management*, vol. 51, no. 12, 2010, pp. 2383-2393.

[8] Yang, Xin-She, and Xingshi He, "Firefly algorithm: recent advances and applications," *International Journal of Swarm Intelligence* 1.1, 2013, pp. 36-50.

[9] Osamu Watande, and Thomas Zeugmann, "Stochastic Algorithms: Foundations and Applications," 5th International Symposium, SAGA 2009 Sapporo, Japan, October 26-28, 2009 Proceedings.

[10] S.M. Al-Alawi, K.A. Ellithy, "Tuning of SVC damping controllers over a wide range of load models using an artificial neural network," *Electrical Power and Energy Systems,* vol. 22,2000, pp. 405-420.

[11] R. C. Bansal and T. S. Bhatti, "Small signal analysis of isolated hybrid power systems: reactive power and frequency control analysis," Narosa Publishing House, New Delhi, India: 2008.

[12] K.R. Padiyar, "Power Systems Dynamics, Stability and Control. Bangalore," India: Interline Publishing, 1996.

[13] O.I. Elgerd, "Electric energy Systems Theory An /introduction", Tata McGraw-Hill Publishing limited, New Delhi, Second Edition 1983

[14] Ray Hunter, Elliot George, Wind-Diesel Systems, A Guide to the technology and its implementation, Cambridge, University Press, 1994**.**

[15] R. C. Bansal, T. S. Bhatti, and D.P. Kothari, "A novel mathematical modeling of induction generator for reactive power control of isolated hybrid power systems," *Int. J. Model. Simul.*, vol. 24, no. 1, 2004, pp. 1-7.